Phase-field model of domain structures in ferroelectric thin films

Y. L. Li, S. Y. Hu, Z. K. Liu, and L. Q. Chen[a)]
Department of Materials Science and Engineering, The Pennsylvania State University, University Park, Pennsylvania 16802

(Received 4 January 2001; accepted for publication 12 April 2001)

A phase-field model for predicting the coherent microstructure evolution in constrained thin films is developed. It employs an analytical elastic solution derived for a constrained film with arbitrary eigenstrain distributions. The domain structure evolution during a cubic→tetragonal proper ferroelectric phase transition is studied. It is shown that the model is able to simultaneously predict the effects of substrate constraint and temperature on the volume fractions of domain variants, domain-wall orientations, domain shapes, and their temporal evolution. © *2001 American Institute of Physics.* [DOI: 10.1063/1.1377855]

A common feature for ferroelectric materials is the formation of domain structures when a paraelectric phase is cooled through the ferroelectric transition temperature called the Curie temperature.[1] The crystallography and thermodynamics of domain structures in bulk systems have been extensively studied and reasonably well understood.[2] The situation can be dramatically different in ferroelectric thin films. The existence of a free surface and substrate constraint destroys the macroscopic symmetry of the system and can significantly affect the relative volume fractions of domains with different orientations and the Curie temperature. Recently, a number of theoretical models have been proposed, which allow the construction of domain stability maps—volume fractions of domains as a function of lattice mismatch with substrate and/or temperature.[3–6] However, due to the analytical nature of the theoretical models, they are focused on the thermodynamics. Moreover, a given domain structure with a particular domain wall orientation has to be assumed as *a priori* in order to determine the volume fractions of domains that minimize the total free energy at a given temperature and substrate constraint.

The main purpose of this letter is to describe a phase-field approach developed for predicting the domain structures in constrained ferroelectric thin films. It does not make any *a priori* assumptions with regard to the possible domain structures that might appear under a given temperature and substrate constraint. It is able to predict not only the effect of substrate constraint on phase transition temperatures and the volume fractions of orientation domains, but also the detailed domain structures and their temporal evolution during a ferroelectric transition. Although similar approaches have been applied to ferroelectric domain evolution in bulk single crystals,[7–9] the presence of a stress-free surface and lattice constraint by the substrate requires an efficient elastic solution for a constrained three-dimensional (3D) film.

We consider a cubic thin film grown heteroepitaxially on a cubic substrate. The film undergoes a cubic-to-tetragonal ferroelectric phase transition below the Curie temperature. For a proper transition, the polarization vector $P=(P_1,P_2,P_3)$ is the primary order parameter and the temporal domain structure evolution is described by the time-dependent Ginzburg–Landau (TDGL) equations[7–9]

$$\frac{\partial P_i(\mathbf{x},t)}{\partial t}=-L\frac{\delta F}{\delta P_i(\mathbf{x},t)},\quad i=1,2,3, \tag{1}$$

where L is the kinetic coefficient related to the domain wall mobility and F is the total free energy of the system. In this work, we ignore any possible surface and interface contributions to the free energy as discussed in Refs. 10 and 11 and assume that the surface of the film is compensated with free charge carriers so the depolarization energy is neglected.

We assume the bulk thermodynamics is characterized by the Landau free energy density expansion,[12]

$$\begin{aligned}f_L(P_i)=&\alpha_1(P_1^2+P_2^2+P_3^2)+\alpha_{11}(P_1^4+P_2^4+P_3^4)+\alpha_{12}(P_1^2P_2^2\\&+P_2^2P_3^2+P_1^2P_3^2)+\alpha_{111}(P_1^6+P_2^6+P_3^6)\\&+\alpha_{112}[P_1^4(P_2^2+P_3^2)+P_2^4(P_1^2+P_3^2)+P_3^4(P_1^2+P_2^2)]\\&+\alpha_{123}(P_1^2P_2^2P_3^2),\end{aligned} \tag{2}$$

where $\alpha_1,\alpha_{11},\alpha_{12},\alpha_{111}\alpha_{112}$, and α_{123} are the expansion coefficients. The contribution of domain walls to the total free energy is introduced through gradients of the polarization field. For a cubic system,

$$\begin{aligned}f_G(P_{i,j})=&\tfrac{1}{2}G_{11}(P_{1,1}^2+P_{2,2}^2+P_{3,3}^2)+G_{12}(P_{1,1}P_{2,2}+P_{2,2}P_{3,3}\\&+P_{1,1}P_{3,3})+\tfrac{1}{2}G_{44}[(P_{1,2}+P_{2,1})^2+(P_{2,3}+P_{3,2})^2\\&+(P_{1,3}+P_{3,1})^2]+\tfrac{1}{2}G'_{44}[(P_{1,2}-P_{2,1})^2\\&+(P_{2,3}-P_{3,2})^2+(P_{1,3}-P_{3,1})^2],\end{aligned} \tag{3}$$

where G_{ij} are gradient energy coefficients. In this letter, a comma in a subscript stands for spatial differentiation, for example, $P_{i,j}=\partial P_i/\partial x_j$. Since the ferroelectric transition involves a structural change, strain appears as a secondary order parameter. The stress-free strain caused by the polarization field is given by[12]

$$\begin{aligned}&\epsilon_{11}^0=Q_{11}P_1^2+Q_{12}(P_2^2+P_3^2),\quad \epsilon_{23}^0=Q_{44}P_2P_3,\\&\epsilon_{22}^0=Q_{11}P_2^2+Q_{12}(P_1^2+P_3^2),\quad \epsilon_{13}^0=Q_{44}P_1P_3,\\&\epsilon_{33}^0=Q_{11}P_3^2+Q_{12}(P_1^2+P_2^2),\quad \epsilon_{12}^0=Q_{44}P_1P_2,\end{aligned} \tag{4}$$

a)Electronic mail: lgc3@psu.edu

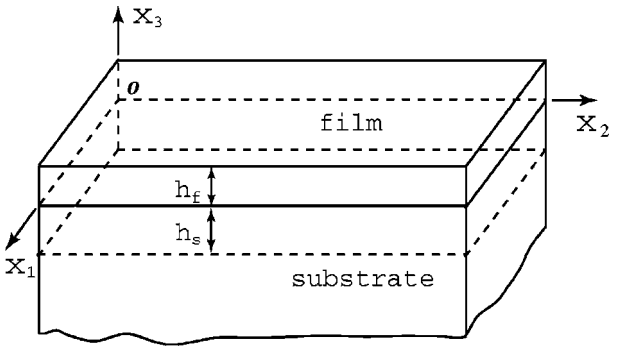

FIG. 1. Schematic illustration of a thin film coherently constrained by a substrate.

where Q_{ij} are the electrostrictive coefficients. If we assume that the interfaces developed during a ferroelectric phase transition as well as the interface between the film and the substrate are coherent, elastic strains e_{ij} and thus elastic strain energy f_E will be generated during the phase transition,

$$f_E=\tfrac{1}{2}c_{ijkl}e_{ij}e_{kl}=\tfrac{1}{2}c_{ijkl}(\epsilon_{ij}-\epsilon^0_{ij})(\epsilon_{kl}-\epsilon^0_{kl}) \equiv f_E(P_i,\epsilon_{ij}), \tag{5}$$

here c_{ijkl} is the elastic stiffness tensor and $\epsilon_{ij}=e_{ij}+\epsilon^0_{ij}$ are the total strains. The summation convention for the repeated indices is employed and $(i,j,k,l,=1,2,3)$.

The total free energy of the film is then $F=\int_V[f_L(P_i)+f_G(P_{i,j})+f_E(P_i,\epsilon_{ij})]d^3x$, where V is the volume of the film. In this model, although both the polarization and strain fields appear as order parameters, one may assume that the mechanical relaxation of an elastic field is faster than that of a polarization field. Consequently, during a ferroelectric transition, one can assume that the system reaches its mechanical equilibrium instantaneously for a given polarization field distribution.

Mechanical equilibrium is satisfied when $\sigma_{ij,j}=0$, where σ_{ij} are the stress components in the film and are given by $\sigma_{ij}=c_{ijkl}e_{kl}=c_{ijkl}(\epsilon_{kl}-\epsilon^0_{kl})$. The mechanical boundary condition for the film is such that its top surface is stress free,

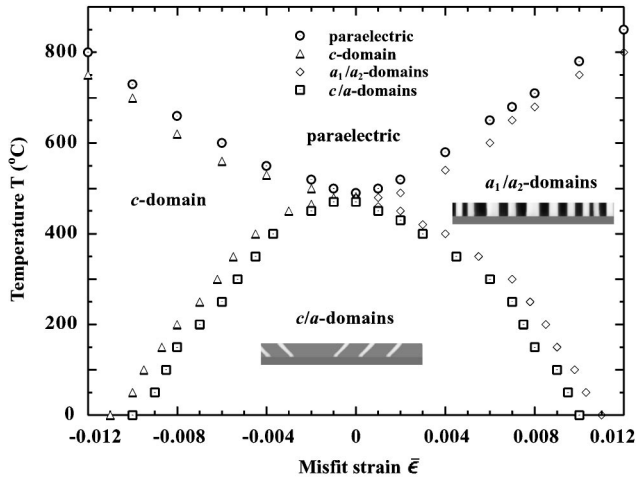

FIG. 2. Domain stability map: domain configuration as a function of substrate constraint and temperature. The two inserts are two-dimensional cross section cuts of the corresponding 3D domain structures obtained from the computer simulations.

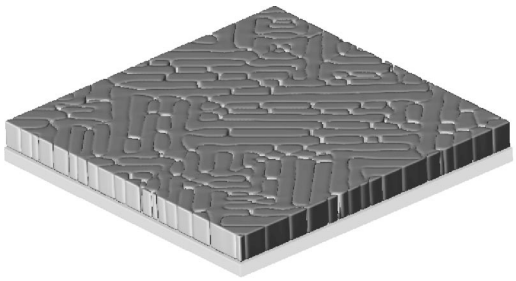

FIG. 3. A predicted domain structure consisting of only a_1 and a_2 domains.

i.e., $\sigma_{i3|x_3=h_f}=0$, where h_f is the film thickness (see Fig. 1), while the bottom surface is coherently constrained. We separate the total strain into a sum of a homogeneous strain and a heterogeneous strain, i.e., $\epsilon_{ij}(\mathbf{x})=\overline{\epsilon_{ij}}+\eta_{ij}(\mathbf{x})$. Consequently, $\sigma_{ij}(\mathbf{x})=\overline{\sigma_{ij}}+s_{ij}(\mathbf{x})$ with $\overline{\sigma_{ij}}=c_{ijkl}\overline{\epsilon_{kl}}$, $s_{ij}(\mathbf{x})=c_{ijkl}[\eta_{kl}(\mathbf{x})-\epsilon^0_{kl}(\mathbf{x})]$. Let $\overline{\epsilon_{\alpha\beta}}$, $(\alpha,\beta=1,2)$ represent the macroscopic shape deformation along the film plane, we have $\int_V\eta_{\alpha\beta}(\mathbf{x})d^3x=0$, $(\alpha,\beta=1,2)$. The other three components $\overline{\epsilon_{i3}}$ meet the requirement that $\overline{\sigma_{i3}}=c_{i3kl}\overline{\epsilon_{kl}}=0$.

To solve the heterogeneous strain η_{ij}, we introduce a set of displacement $u_i(\mathbf{x})$ through $\eta_{ij}=\frac{1}{2}(u_{i,j}+u_{j,i})$. The equations of mechanical equilibrium can be rewritten as

$$c_{ijkl}u_{k,lj}=c_{ijkl}\epsilon^0_{kl,j}, \tag{6}$$

with the boundary condition on the top surface changed to

$$c_{i3kl}(u_{k,l}-\epsilon^0_{kl})|_{x_3=h_f}=0. \tag{7}$$

Since the elastic perturbation in the substrate disappears far away from the film–substrate interface, one can define another boundary condition, i.e.,

$$u_i|_{x_3=-h_s}=0, \tag{8}$$

where h_s is the distance from the interface into the substrate, beyond which the elastic deformation can be ignored (see Fig. 1). In this work, the elastic properties of the film and the substrate are taken to be homogeneous. Equations (6)–(8) were solved by combining a solution for a 3D full space, subject to the body force $f_i=c_{ijkl}\epsilon^0_{kl,j}$, and a solution for an infinite plate of thickness h_f+h_s without body force. The details will be given in a future article.

We use lead titanate ($PbTiO_3$) thin film as an example for our numerical simulations. We solved the TDGL Eq. (1) employing the semi-implicit Fourier-spectral method.[13] The material constants for the Landau free energy and the electrostrictive coefficients can be found in Refs. 14 and 15: $\alpha_1=3.8(T-479)\times10^5$, $\alpha_{11}=-7.3\times10^7$, $\alpha_{12}=7.5\times10^8$,

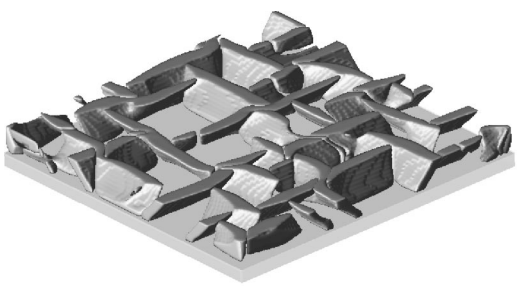

FIG. 4. 3D representation of a_1 and a_2 domains for the case with about 65% c domains.

TABLE I. Volume fraction of c domains, V_c, as a function of $\bar{\epsilon}$.

$\bar{\epsilon}$	−0.012	−0.008	−0.006	−0.004	−0.02	0.0	0.002	0.006	0.012
V_c	1.0	0.97	0.901	0.832	0.751	0.646	0.539	0.261	0.0

$\alpha_{111}=2.6\times10^8$, $\alpha_{112}=6.1\times10^8$, $\alpha_{123}=-3.7\times10^9$, $Q_{11}=0.089$, $Q_{12}=-0.026$, and $Q_{44}=0.03375$, ub Si units and is temperature T in °C. The elastic properties are assumed to be isotropic. The elastic shear modulus and Poisson's ratio are taken as $\mu=0.4762\times10^{11}$ $m^{-2}N$ and $\nu=0.312$. In the computer simulations, we defined reduced units following Ref. 8. In the reduced units, the gradient energy coefficients are $G_{11}/G_{110}=0.6$,$G_{12}/G_{110}=0.0$, and $G_{44}/G_{110}=G'_{44}/G_{110}=0.3$. We employed $128\times128\times36$ discrete grid points and periodic boundary conditions are applied along the x_1 and y_2 axes. The grid spacing in real space is chosen to be $\Delta x_1/l_0=\Delta x_2/l_0=1.0$ and $\Delta x_3/l_0=0.5$, where $l_0=\sqrt{G_{110}/\alpha_0}$ and $\alpha_0=|\alpha_1|_{T=25\,^\circ C}$. Based on recent experimental measurements,[16,17] G_{110} is about $0.9–6.8(\times10^{-10}$ $C^{-2}m^4N)$, which corresponds to a 90° domain-wall energy of 0.04–0.12 (Nm^{-1}) and the length scale $l_0=0.7–2.0$ (nm). With these values, the domain wall width in our simulations is about 1.1–4.0 (nm), which agree well with experimental measurements.[17] The time step for integration is $\Delta t/t_0=0.03$, where $t_0=1/(\alpha_0 L)$.

The effect of substrate constraint and temperature on the domain volume fractions is summarized in the domain stability map (Fig. 2). The effect of the substrate is controlled by changing the macroscopic average strain $\bar{\epsilon}_{\alpha\beta}$. We consider the simple case of a cubic substrate with the [001] orientation, and hence $\bar{\epsilon}_{11}=\bar{\epsilon}_{22}=\bar{\epsilon}$ and $\bar{\epsilon}_{12}=0$. We choose a value of $h_s=12\Delta x_3=0.6h_f$, beyond which our simulations showed little changes in the results.[18] Depending on the substrate constraint and temperature, the low temperature ferroelectric state may possess one of the three possible domain configurations. We use a_1 and a_2 to label the domains with their tetragonal axes along the film plane and c to label; the domains with its tetragonal axis perpendicular to the film surface. Under a large compressive substrate constraint, the equilibrium domain configuration is a single c domain with 180° domain walls. On the other hand, for a large tensile substrate constraint, a_1 and a_2 domains dominate. An example of a domain structure for $\bar{\epsilon}=0.02$ at $T=25$°C is shown in Fig. 3 in which only a_1 and a_2 domains exist. In Fig. 3, only the domain walls are shown and the a_1 domains and a_2 domains are not distinguished. Essentially all the domain walls are perpendicular to the film surface and along the [110] or [1$\bar{1}$0] directions. The domain structures with a moderate compressive or very small tensile stress are dramatically different from that in Fig. 3. An example of a domain structure obtained for the case of $\bar{\epsilon}=0.0$ at $T=25$°C is shown in Fig. 4. The volume fraction of c domains is roughly 0.65. The a_1 and a_2 domains are plates aligning about 45° from the substrate (the c domains are not shown in Fig. 4). The a_1- and a_2-domain orientation and shapes predicted from the simulations agree very well with existing experimental observations[19,20] for a compressive substrate constraint. At $T=25$ °C, the volume fraction of c domains, V_c, as a function of mismatch strain is given in Table I. It is shown that the substrate constraint can dramatically alter the volume fractions of different orientation domains. The volume fraction of c domains decreases as the magnitude of $\bar{\epsilon}$ increases and there are no c domains when $\bar{\epsilon}=0.012$ or larger (also see Fig. 2).

It should be emphasized that although the domain stability map shown in Fig. 2 is similar to that obtained from a thermodynamic analysis,[6] there are two important differences. First, the approach presented here does not require any *a priori* assumption on the possible domain wall orientations for predicting the domain stability map. All the data points shown in Fig. 2 were obtained by starting from an initial paraelectric state. As a result, the a_1/a_2 domain configurations under a large tensile substrate constraint were automatically predicted using the proposed approach whereas in the thermodynamic analysis, a domain configuration consisting of a rhombohedral phase and a tetragonal a-phase was obtained under a similar tensile substrate constraint.[6] Second, the proposed approach allows the prediction of domain shapes and spatial arrangement as well as their temporal evolution. Therefore, it is possible to study domain nucleation and growth as well as the domain wall motion under an applied field, i.e., domain switching.

The authors are grateful for the financial support from the National Science Foundation under Grant No. DMR 96-33719.

[1] M. E. Lines and A. M. Glass, *Principles and Applications of Ferroelectrics and Related Materials* (Clarendon, Oxford, 1977).
[2] G. Arlt, Ferroelectrics **104**, 217 (1990).
[3] J. S. Speck and W. Pompe, J. Appl. Phys. **76**, 466 (1994).
[4] A. L. Roytburd, J. Appl. Phys. **83**, 228 (1998).
[5] A. L. Roytburd, J. Appl. Phys. **83**, 239 (1998).
[6] N. A. Pertsev, V. G. Koukhar, Phys. Rev. Lett. **84**, 3722 (2000).
[7] S. Nambu and D. A. Sagala, Phys. Rev. B **50**, 5838 (1994).
[8] H. L. Hu and L. Q. Chen, J. Am. Ceram. Soc. **81**, 492 (1998).
[9] S. Semenovskaya and A. G. Khachaturyan, J. Appl. Phys. **83**, 5125 (1998).
[10] K. Binder, Ferroelectrics **35**, 99 (1981).
[11] D. R. Tilley and B. Zeks, Solid State Commun. **49**, 823 (1984).
[12] A. F. Devonshire, Philos. Mag., Suppl. **3**, 85 (1954).
[13] L. Q. Chen and J. Shen, Comput. Phys. Commun. **108**, 147 (1998).
[14] M. J. Haun, E. Furman, S. J. Jang, H. A. Mckinstry, and L. E. Cross, J. Appl. Phys. **62**, 3331 (1987).
[15] N. A. Pertsev, A. G. Zembilgotov, and A. K. Tabantev, Phys. Rev. Lett. **80**, 1988 (1998).
[16] S. Stemmer, S. K. Streiffer, F. Ernst, and M. Rühle, Philos. Mag. A **71**, 1988 (1995).
[17] M. Foeth, thesis, Ecole Polytechnique Federal de Lausanne, 1999.
[18] Y. L. Li, S. Y. Hu, Z. K. Liu, and L. Q. Chen, MRS 2000 Fall Symposium Y Proceedings, 2000.
[19] A. Seifert, F. F. Lange, and J. S. Speck, J. Mater. Res. **10**, 680 (1995).
[20] S. P. Alpay, V. Nagarajan, L. A. Bendersky, M. D. Vaudin, S. Aggarwal, R. Ramesh, and A. L. Roytburd, J. Appl. Phys. **85**, 3271 (1999).